High Temperature Sulphidation of Cast Austenitic Alloy Cr25-Ni32-Nb with Microadditives Ti, Zr and Ce

Renata Zapała[1], Zbigniew Zurek[2], Jan Głownia[1]

[1] *AGH University of Science and Technology, Faculty of Foundry Engineering, al. Mickiewicza 30, 30-059 Cracow, Poland*

[2] *Cracow University of Technology, Faculty of Chemical Engineering and Technology, Warszawska street 24, 31-155 Cracow, Poland*

(Received April 15,2008:final form May 13,2008)

ABSTRACT

This work presents the results of a study of cast austenitic alloy Cr25-Ni32-Nb, with microadditives (Ti, Zr, Ce) sulphidated at 1073K in H_2/H_2S atmosphere, the exposure time being 25 hours. The samples under investigation were cut out from the centrifugally cast tubes: columnar and equiaxed grains zones. Some minor differences were found between the sulphidation rate of specimens from the equiaxed grains and columnar grains zones. Additionally, morphological studies of scales formed on the investigated alloys were conducted, showing a change in the volume fraction of niobium and chromium carbides. The volume fraction of niobium and chromium carbides proved to be considerably higher in the material exposed to sulphidation than in the starting material.

1. INTRODUCTION

Catalytic conversion of methane by steam belongs to endothermic processes. To ensure the temperature of 1093 – 1423K in the reaction zone, tubing which is an essential part of the installation, is heated by gas burners located on furnace walls /1/. The fuel used in industry, natural gas, is usually contaminated with sulphur or sulphur-bearing species, which significantly accelerate degradation of the outer surface of catalytic converter tubing /2-5/. The degradation is directly related to the formation of sulphide scales, which for many metals is much faster compared with oxide scales. Moreover, the corrosion process can be enhanced by low-melting metal-metal sulphide eutectics (e.g. melting point of the Ni_3S_2-Ni eutectic is as low as 918K) /3 - 7/.

Refractory metals, such as Nb, Mo and V behave differently /4/. When introduced as alloying additions, these metals can reduce the rate of sulphidation of structural materials used in the manufacturing of catalytic converter tubing /5/. The sulphidation resistance of scaling resistant alloys due to Nb, Mo and V additives, is generally only slightly improved. Materials, which exhibit relatively good resistance to sulphur, are austenitic steels.

The multiphase sulphide scales on austenitic steels are built of one, two or three layers /6-7/. The outer layer consists of FeS doped with chromium, the intermediate one of sulphospinel, $FeCr_2S_4$, and the inner one of (Fe,Cr)S and $FeCr_2S_4$. As the diffusion of metals in $FeCr_2S_4$ is much slower than in (Fe,Cr)S, the appearance of a sulphospinel layer in the scale brings about reduction of sulphidation rate /6-8/. Big pores observed in the $FeCr_2S_4$ scale on austenitic steels (e.g. Fe-Cr18-Ni10 with Ti) grow in size upon exposure /8/.

The present work is an attempt to identify the role of microadditives in a scaling resistant austenitic alloy, Cr25-Ni32-Nb, centrifugally cast, and the interrelations between alloy microstructure, sulphidation kinetics, morphology of the external scale and of the internal sulphidation zone.

2. EXPERIMENTAL

The experimental alloy, Cr25-Ni35-Nb, was centrifugally cast in laboratory conditions. The microstructure of tubular castings differed on the cross-section. The specimens were cut out in the areas of columnar crystals and of equiaxed crystals (Fig. 1). All experimental alloys were melted in an induction furnace, capacity of 100 kg. Prior to melting the metallic charge composed of Cr-Ni and Ni scrap was placed in monolythic acid crucibles. Other components (Fe-Cr, Fe-Mn) were added to the molten metal bath after deoxidizing treatment. Next the chemical composition of molten metal bath was analysed. After removal of slag and consecutive deoxidizing treatment, the desired chemical composition was adjusted by introduction of Ni, Fe-Cr, Fe-Mn and Fe-Nb. The temperature of tapping was 1823-1873K. Once the temperature was read-out, molten metal was tapped to a hand ladle, 20 kg in capacity. The composition of alloy was adjusted in the ladle by introducing alloying additions together with deoxidising agents (Al - 1 kg/Mg and Fe-Ca-Si – 1.5 kg/Mg). The modifiers were: Ti [as Fe-Ti alloy (72% Ti)], Zr [as Fe – Si – Zr alloy (38% Zr and 49% Si)], rare-earth metals as Mischmetal (ab. 50 % Ce) and pure Ce. The experimental alloy had austenitic structure with carbide precipitates along the grain boundaries and inside the grains. The carbide phases identified were NbC, $Cr_{23}C_6$ and Cr_7C_3 /9, 10/.

Chemical compositions of the investigated alloys together with the adopted symbols are given in **Table 1**.

Table 1

Chemical composition of experimental alloys.

Samples notation		Chemical composition [mass %]									
		C	Si	Mn	Cr	Ni	Nb	Mo	Ti	Zr	Ce
A	1_r	0.29	1.99	1.06	24.99	30.82	1.16	0.17	-	-	-
	2_s										
B	1_r	0.28	2.15	0.97	24.62	30.89	1.12	0.16	0.075	0.083	-
	2_s										
C	1_r	0.29	2.44	0.88	24.22	31.38	1.13	0.16	0.12	0.082	-
	2_s										
D	1_r	0.28	2.12	0.97	24.41	31.26	1.14	0.16	0.069	0.083	0.064
	2_s										
E	1_r	0.28	2.04	0.99	24.32	31.77	1.17	0.17	-	-	0.16
	2_s										
r – equiaxed grains, s –columnar grains											

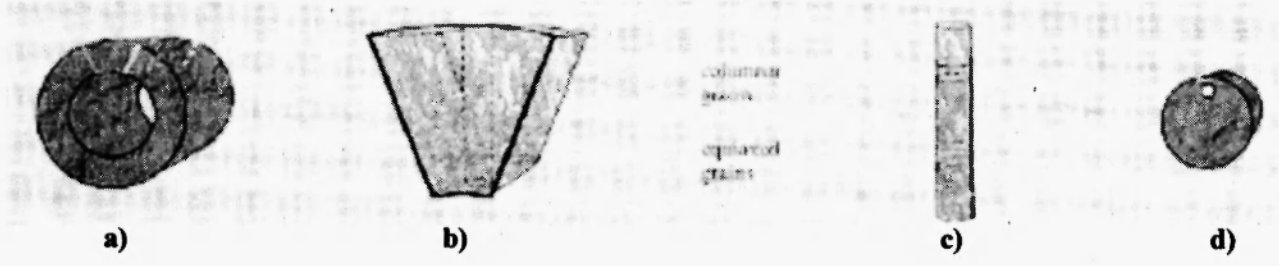

Fig. 1: Scheme of specimen preparation for sulphidation experiments: a – tubular casting; b – columnar and equiaxed structure on casting cross-section; c – segment of casting used for test specimens (d).

A scheme of specimen preparation is presented in **Fig. 1**. The test specimens were flat discs, 6mm in diameter and about 1mm in thickness, cut out in the area of columnar and equiaxed grains. The equiaxed grains differed in size. The average grain diameter varied between 0.041 and 0.084 mm, depending on alloy composition. The columnar grains were ten times larger. Small holes, 0.5 in diameter, were drilled in the specimens for suspension. The specimens were polished to a mirror-like lustre, degreased in water with detergent in ultrasonic bath. Subsequently the specimens were washed with ethanol and dried in a stream of warm air.

The sulphidation experiments were conducted at 1073K, in a H_2/H_2S mixture (total pressure of 1 atm) with sulphur partial pressure of p_{S_2} = 10^{-8} atm = 10^{-3} Pa. The exposure time was 25 hours (90 000 s).

The surface of scales was examined under a light microscope, NEOPHOT 32. The morphology and chemical composition of precipitates were analysed by scanning electron microscope JEOL 5500LV (maximum resolution of 4 nm, magnification 18 – 30000x), with an X-ray microanalyser IXRF EDS. The phase composition was determined by means of a Siemens Kristalloflex 4H diffractometer, using Cu_α radiation. Diffraction lines were recorded in the 2θ range of 20° - 90°. The XRAYAN software was used for data processing.

3. RESULTS AND DISCUSSION

Sulphidation of the Cr25-Ni32-Nb cast alloys is presented in **Fig. 2(a)** and **2(b)**.

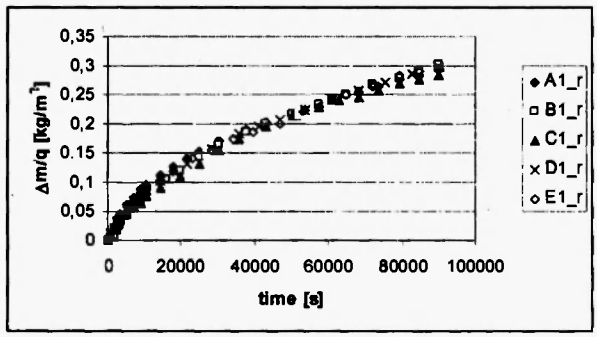

Fig. 2a: Sulphidation of the Cr25-Ni35-Nb alloy in a H_2/H_2S mixture at $pS_2 = 10^{-8}$ atm = 10^{3} Pa and 1073K, specimen with equiaxed grains.

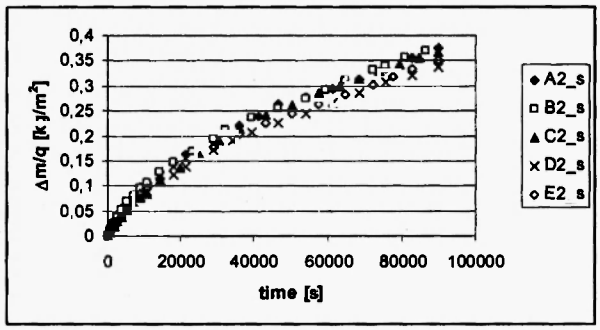

Fig. 2b: Sulphidation of the Cr25-Ni35-Nb alloy in a H_2/H_2S mixture at $pS_2 = 10^{-8}$ atm = 10^{-3} Pa and 1073K, specimen with columnar grains.

The measurements of sulphidation kinetics of the Cr25-Ni35-Nb alloys indicate approximately parabolic behaviour. The exponent in the kinetic equation for the specimens with equiaxed grains varied in the range 1.42 – 1.61, and for the specimens with columnar grains n = 1.27 – 1.49. Significant differences were found between the values of Δm/q for the specimens with columnar grains and specimens with equiaxed grains.

Table 2
Values of k_p for the investigated alloys

Samples	Values of $k_p [kg^2/(m^4 \cdot s^1)]$	
	1_r	2_s
A	$9.48 \cdot 10^{-7}$	$1.47 \cdot 10^{-6}$
B (Ti+Zr)	$9.67 \cdot 10^{-7}$	$1.49 \cdot 10^{-6}$
C (Ti+Zr)	$9.37 \cdot 10^{-7}$	$1.43 \cdot 10^{-6}$
D (Ti+Zr+Ce)	$9.56 \cdot 10^{-7}$	$1.18 \cdot 10^{-6}$
E (Ce)	$9.49 \cdot 10^{-7}$	$1.28 \cdot 10^{-6}$

The order of magnitude of the parabolic rate constant was essentially the same for specimens with different compositions but the same microstructure (equiaxed or columnar grains). A difference of about one order of magnitude was found between the sulphidation rate of specimens of the same material with equiaxed grains (r) and with columnar grains (s). The former sulphidised more slowly than the latter. Due to the higher density of grain boundaries in the alloy with the equiaxed grains, the grain-boundary diffusion of Cr is enhanced and the slowly growing phases, $FeCr_2S_4$ and

FeS Cr_2S_3, are favoured (Leistikow effect) /11/.

Morphological studies of the sulphidised specimens were conducted by means of a light microscope. **Figure 3** shows the surface of sulphide scales on the baseline alloy (A) and on the modified alloys (B, C, D and E). It has been found that the structure of scales formed on all investigated alloys is related to that of the underlying alloy. The grain sizes of scales on specimens with columnar grains are similar (see Fig.3) and the scale formed on specimens with equiaxed grains is fine-grained, similarly as the sulphidised alloy. On the surface of scale there were irregular bands of crystals oriented perpendicularly to the grain boundaries of the alloy (**Fig. 4**). According to EDS, the outgrowing crystals are built of Fe and S and small amounts of Cr. The X-ray diffraction measurements indicated $Fe_{1-x}S$ (**Fig. 5**). The scale surface is discontinuous, with visible porosity and cracks propagating along the grain boundaries and across the grain boundaries (**Fig. 6**). Phases identified are $FeCr_2S_4$ and FeS Cr_2S_3.

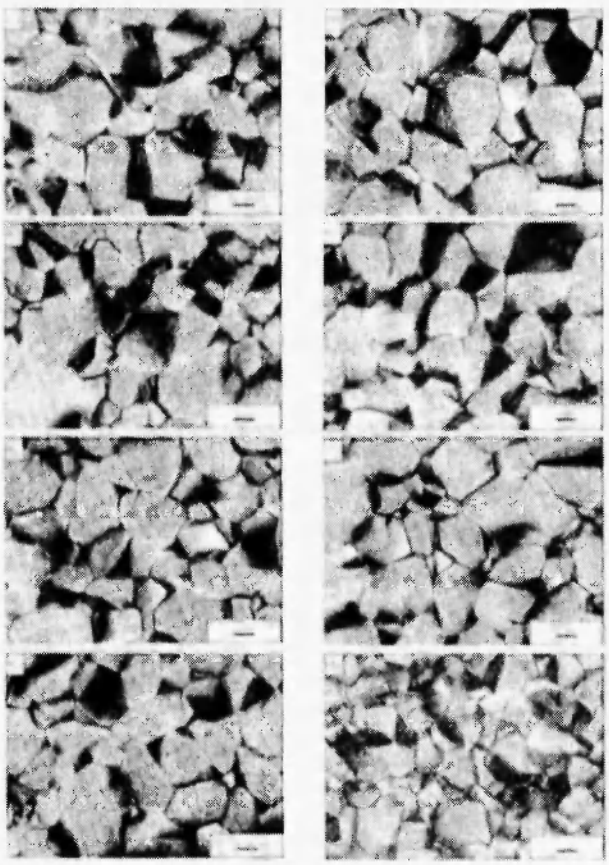

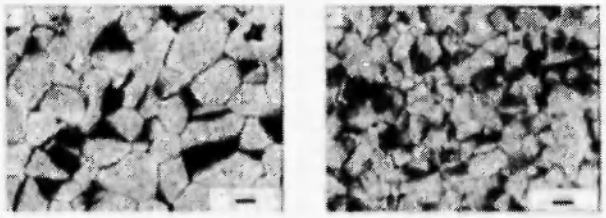

Fig. 3: Surface of specimen sulphidised at 1073K for 25 h (90 000 s) (light microscope).

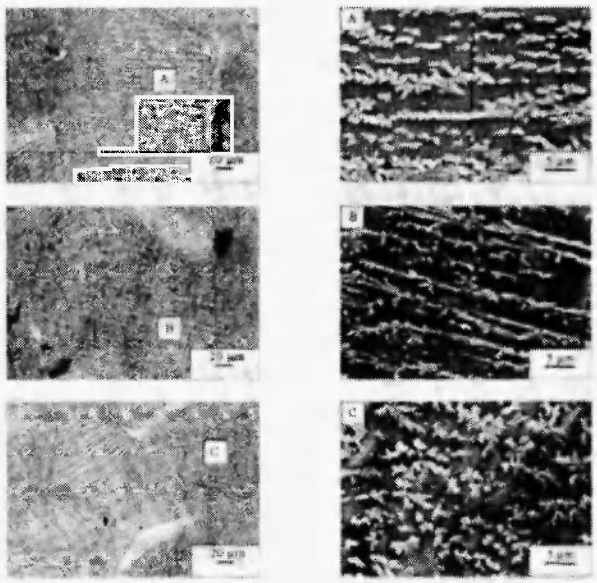

Fig. 4: Outgrowths of $Fe_{1-x}S$ on the surface the sulphidised alloy B (Ti+Zr); SEM images at different magnifications.

Fig. 5: Diffraction pattern of alloy A.

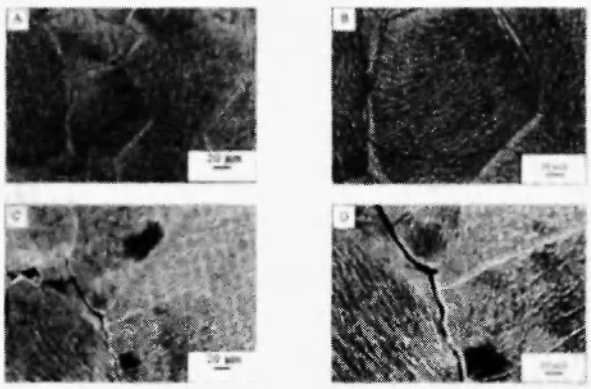

Fig.6: Cracks and pores on scale surface on alloy B (SEM images at different magnifications).

The sulphide scales formed on all alloys studied are not adherent and tend to spall upon cooling. The only exception is cast steel grade stabilised with Ce, which shows relatively good adherence. The poor adherence of scales is caused by the formation of volatile products of reactions between hydrogen and carbon from niobium carbides in the internal sulphidation zone beneath the alloy/scale interface. **Figure 7** presents sulphide scales on specimens E2_s and D2_s. As follows from the observation of specimen cross-sections, the scale is composed of a single-layer with significant porosity; pores being located mainly next to the scale/alloy interface.

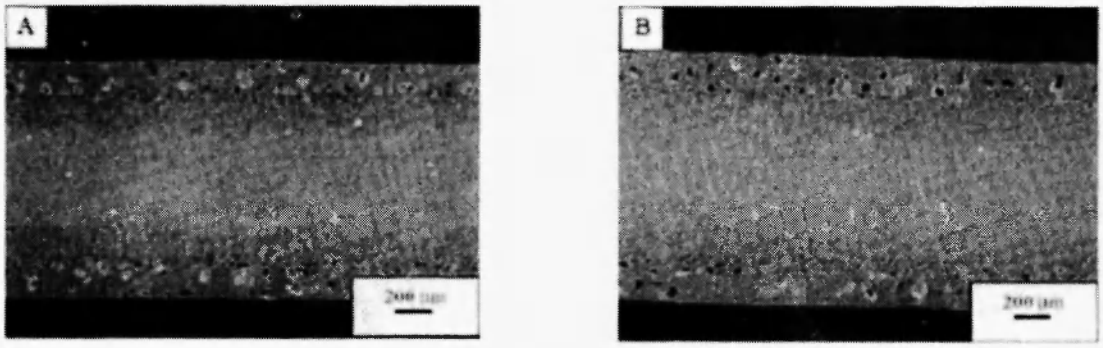

Fig. 7: Cross-sections of sulphidised specimens D2_s (a) and E2_s (b) (SEM images).

Figure 8 shows a cross-section of the sulphidised specimen of alloy A. EDS and X-ray diffraction analyses indicate that the coarse-grained scale on all alloys studied consists of $Fe_{1-x}S$, $FeCr_2S_4$ and $FeS{\cdot}Cr_2S_3$ (see **Fig. 9**). The outermost part of the scale is built of $Fe_{1-x}S$, while $FeCr_2S_4$ and FeS Cr_2S_3 are components of the inner part and of the layer next to the metallic core. Under the scale, there is an internal sulphidation zone with $FeCr_2S_4$ precipitates in the Ni-rich matrix (up to 69 mass% Ni), which is Cr-depleted and contains fine precipitates of Nb carbides. The Ni enrichment in this zone can be explained by the fact that the suphidation experiments were conducted under sulphur pressure lower than the dissociation pressure of nickel sulphides.

In the starting alloys, niobium was present in the form of NbC or complex carbides containing Nb, Ti and Zr when the alloys were modified with titanium and zirconium. Some chromium carbides - $Cr_{23}C_6$ – were also found. **Figures 10** and **11** demonstrate volume fractions of niobium and chromium carbides in the internal sulphidation zone and in the subjacent alloy A with equiaxed and columnar grains, respectively. The internal sulphidation zone was practically free of chromium carbides but contained some dispersed niobium carbides. This can be explained by higher stability of niobium carbides compared to chromium carbides /12, 13/. At the front of the internal sulphidation zone, the volume fraction of chromium sulphides and niobium sulphides is much lower than in the starting material. In contrast, the volume fraction of niobium carbides and particularly chromium carbides is increased beneath the internal sulphidation zone (**Figs. 9**, 10 and 11), amounting to about 3-4%. This change in carbides distribution over the specimen cross-section after exposure is consistent with the degradation mechanism of the ferritic steel, type 9Cr-lMo /14/. As earlier reported /11,14/, in presence of sulphur the stability of carbide phases, particularly of $Cr_{23}C_6$, decreases. Sulphur present on the surface and in

subsurface area of the 9Cr-Mo steel makes the activity of carbon increase, which triggers inward diffusion of this element. As practically all niobium in the alloy is bonded in NbC precipitates, the consequence of carbon inward diffusion is increasing volume fraction of chromium carbide $Cr_{23}C_6$ in the alloy. The observed differences are small but confirm the degradation mechanism proposed in /12, 13/.

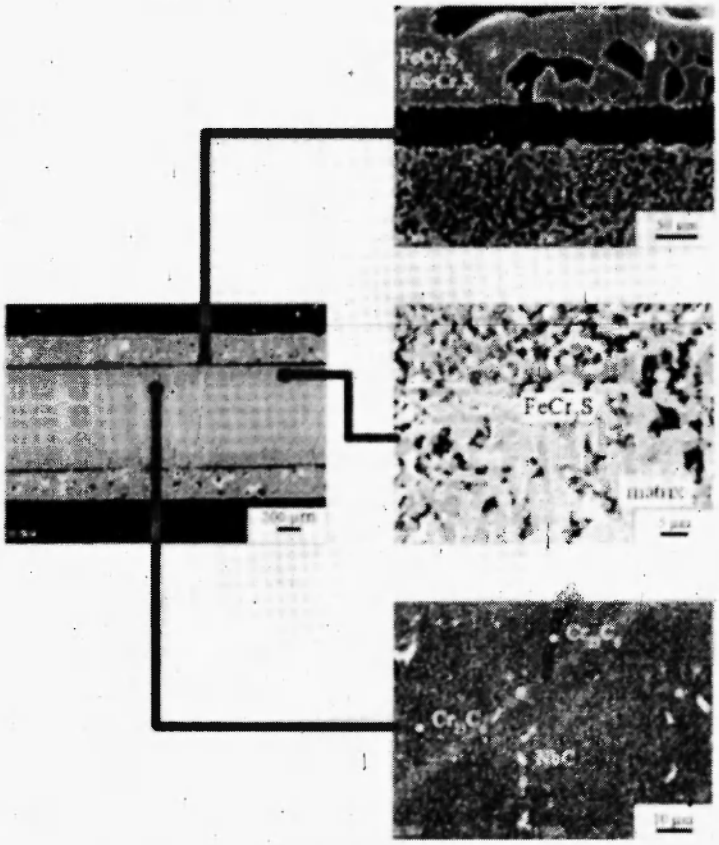

Fig.8: Cross-section of alloy A2_s specimen after sulphidation in H_2/H_2S mixture at 1073K for 25 hours (90000 s) (SEM image).

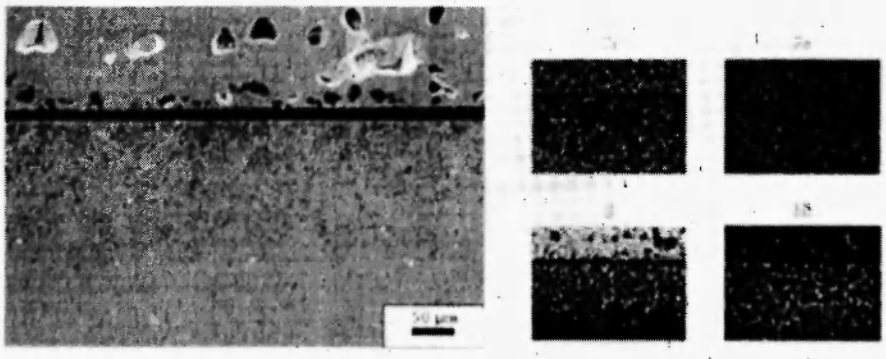

Fig. 9: Cross-section of sulphide scale on alloy A2_s (SEM image with EDS mapping).

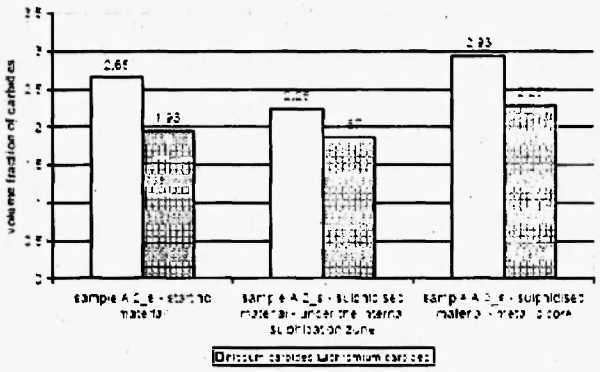

Fig. 10: Volume fraction of carbides in starting material A1_r (with equiaxed grains).

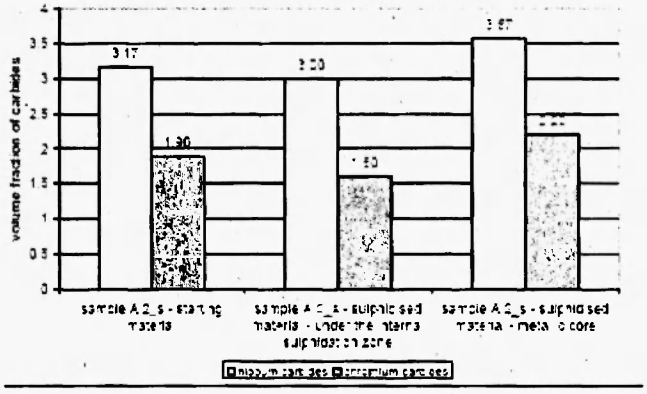

Fig. 11: Volume fraction of carbides in starting material A2_s (with columnar grains).

Table 3 lists the data on average widths of the external scale and of the internal sulphidation zone. The measurements were made on specimen cross-sections upon SEM analysis. The internal sulphidation zone was generally thicker than the external scale. Specimens with equiaxed grains had the internal sulphidation zone thinner by about 15-20%, compared to the specimens with columnar grains.

In specimens modified with Ti, Zr and Ce, the internal sulphidation zone was thicker by about 20% than in baseline alloy specimens. The investigations carried out in this work indicate that alloying additions with higher affinity for sulphur, influence the extent of internal sulphidation.

Table 3
Average width of the external scale and the internal sulphidation zone on the investigated materials.

Samples notation		Average width of the internal sulphidation zone [μm]	Average width of the external scale [μm]
A	1_r	143.1	-
	2_s	165.4	155.2
B	1_r	197.6	130.4
	2_s	205.5	-
C	1_r	168.6	139.9
	2_s	225.9	188.8
D	1_r	160.1	-
	2_s	204.3	168.3
E	1_r	180.7	-
	2_s	210.3	181.3

* the width of the internal sulphidation zone calculated on the basis of measurements which were made on 5 areas of each sample

4. CONCLUSIONS

1. Microstructure can influence the sulphidation rate of the investigated materials to some extent: for the specimens with equiaxed grains the sulphidation rate was about ten times lower than for the specimens with columnar grains; differences being more pronounced after a longer exposure time.
2. Alloy microstructure affects the extent of the internal sulphidation zone.
3. Type and concentration of alloying additions significantly modify morphology of the external scale. When Ce or Ti+Zr+Ce are present in the alloy, the sulphide scales are fine-grained.
4. Combination of three additives, Ti+Zr+Ce, and cerium alone brings about improved scale adherence.
5. Beneath the internal sulphidation zone, the volume fraction of chromium carbides in the alloy increases.

REFERENCES

1. D.J. Tillack and J.E. Guthrie, *Wrought and Cast Heat-Resistant Stainless Steels and Nickel Alloys for the Refining and Petrochemical Industries*, NiDI Technical series 10071 Nickel Development Institute Toronto (1992).
2. J. Labanowski, *Ocena parametrów niszczenia rur katalitycznych w eksploatacji reformerów metanu*, Wyd. Politechniki Gdańskiej, Gdansk (2003).
3. A.J. Sedriks, *Corrosion of Stainless Steels*, Wiley & Sons, New York (1996).
4. S. Mrowec and K. Przybylski, *High. Temp. Mater. Process.*, 6, (1/2), 1-79 (1984).
5. B. Mikułowski, *Stopy zaroodporne i zarowytrzymale. Nadstopy*, Wyd. Akademii Górniczo-Hutniczej Kraków (1997).
6. W. Grosser, D. Meder, W. Auer and H. Kaesche, *Werkst Korros.*, **43**, (4), 145-153 (1992).
7. F. Gesmundo, F. Viani, W. Znamirowski, K. Godlewski and F. Bregani, *Werkst. Korros.*, **43**, (3), 83-95 (1992).
8. M. Schulte, A. Rahmel and M. Schutze, *Oxid. Met.*, **49**, (1/2), 33-70 (1998).
9. R. Zapała, J. Głownia, W. Ratuszek and G. Tęcza, *Polska Metalurgia w latach 2002-2006*, edited by K. Światowski, Wyd. Naukowe AKAPIT, Kraków, (2006) 431-436.
10. .Z. Chen, C.W. Thomas and D.M. Knowles, *Mater. Sci. Eng. A*, **374**, (1/2), 398-408 (2004).
11. S. Leistikow, I. Wolf and H.J. Grabke, *Werkst. Korros.*, **38**, (10), 556-562 (1987).
12. H.J Goldschmidt, *Interstital Alloy*, Butterworths, London, (1967)
13. L.A. Dobrzynski, *Materiały inzynierskie i projektowanie materialowe*, Wyd. Naukowo-Techniczne, Warszawa, (2006).
14. J. Hucińska, *Degradacja stali w środowiskach pieców rafinacyjnych*, Wyd. Politechniki Gdańskiej, Gdansk (2003).